

# Radioisotopic Purity of Sodium Pertechnetate $^{99m}\text{Tc}$ Produced with a Medium-Energy Cyclotron: Implications for Internal Radiation Dose, Image Quality, and Release Specifications

Svetlana V. Selivanova<sup>1,2</sup>, Éric Lavallée<sup>1</sup>, Helena Senta<sup>1</sup>, Lyne Caouette<sup>1</sup>, Jayden A. Sader<sup>3</sup>, Erik J. van Lier<sup>3</sup>, Alexander Zyuzin<sup>3</sup>, Johan E. van Lier<sup>1,2</sup>, Brigitte Guérin<sup>1,2</sup>, Éric Turcotte<sup>1,2</sup>, and Roger Lecomte<sup>1,2</sup>

<sup>1</sup>Sherbrooke Molecular Imaging Center, CRCHUS, Sherbrooke, Quebec, Canada; <sup>2</sup>Department of Nuclear Medicine and Radiobiology, Faculty of Medicine and Health Sciences, Université de Sherbrooke, Sherbrooke, Quebec, Canada; and <sup>3</sup>Advanced Cyclotron Systems Inc., Richmond, British Columbia, Canada

Cyclotron production of  $^{99m}\text{Tc}$  is a promising route to supply  $^{99m}\text{Tc}$  radiopharmaceuticals. Higher  $^{99m}\text{Tc}$  yields can be obtained with medium-energy cyclotrons in comparison to those dedicated to PET isotope production. To take advantage of this capability, evaluation of the radioisotopic purity of  $^{99m}\text{Tc}$  produced at medium energy (20–24 MeV) and its impact on image quality and dosimetry was required. **Methods:** Thick  $^{100}\text{Mo}$  (99.03% and 99.815%) targets were irradiated with incident energies of 20, 22, and 24 MeV for 2 or 6 h. The targets were processed to recover an effective thickness corresponding to approximately 5-MeV energy loss, and the resulting sodium pertechnetate  $^{99m}\text{Tc}$  was assayed for chemical, radiochemical, and radionuclidic purity. Radioisotopic content in final formulation was quantified using  $\gamma$ -ray spectrometry. The internal radiation dose for  $^{99m}\text{Tc}$ -pertechnetate was calculated on the basis of experimentally measured values and biokinetic data in humans. Planar and SPECT imaging were performed using thin capillary and water-filled Jaszczak phantoms. **Results:** Extracted sodium pertechnetate  $^{99m}\text{Tc}$  met all provisional quality standards. The formulated solution for injection had a pH of 5.0–5.5, contained greater than 98% of radioactivity in the form of pertechnetate ion, and was stable for at least 24 h after formulation. Radioisotopic purity of  $^{99m}\text{Tc}$  produced with 99.03% enriched  $^{100}\text{Mo}$  was greater than 99.0% decay corrected to the end of bombardment (EOB). The radioisotopic purity of  $^{99m}\text{Tc}$  produced with 99.815% enriched  $^{100}\text{Mo}$  was 99.98% or greater (decay corrected to the EOB). The estimated dose increase relative to  $^{99m}\text{Tc}$  without any radionuclidic impurities was below 10% for sodium pertechnetate  $^{99m}\text{Tc}$  produced from 99.03%  $^{100}\text{Mo}$  if injected up to 6 h after the EOB. For 99.815%  $^{100}\text{Mo}$ , the increase in effective dose was less than 2% at 6 h after the EOB and less than 4% at 15 h after the EOB when the target was irradiated at an incident energy of 24 MeV. Image spatial resolution and contrast with cyclotron-produced  $^{99m}\text{Tc}$  were equivalent to those obtained with  $^{99m}\text{Tc}$  eluted from a conventional generator. **Conclusion:** Clinical-grade sodium pertechnetate  $^{99m}\text{Tc}$  was produced with a cyclotron at medium energies. Quality control procedures and release specifications were drafted as part of a clinical trial application that received approval from Health Canada. The results of this work are intended to contribute to establishing a regulatory framework for using cyclotron-produced  $^{99m}\text{Tc}$  in routine clinical practice.

**Key Words:**  $^{99m}\text{Tc}$ -pertechnetate; cyclotron; radionuclidic and radioisotopic purity; dosimetry; imaging

**J Nucl Med 2015; 56:1600–1608**

DOI: 10.2967/jnumed.115.156398

The radioisotope  $^{99m}\text{Tc}$  remains indispensable in nuclear imaging.  $^{99m}\text{Tc}$  is usually obtained from generators containing the mother isotope,  $^{99}\text{Mo}$ , which in turn is made from highly enriched  $^{235}\text{U}$  ( $\geq 20\%$ , typically 93%) in nuclear reactors.  $^{99m}\text{Tc}$  is eluted in the form of sodium pertechnetate and can be used as is or as the starting material for other  $^{99m}\text{Tc}$  radiopharmaceuticals used in a variety of diagnostic applications. Cyclotron production of  $^{99m}\text{Tc}$  could be a viable alternative or a complement to the current supply chain of  $^{99m}\text{Tc}$  radiopharmaceuticals. The amount of  $^{99m}\text{Tc}$  produced using a conventional medical cyclotron operating at 16–18 MeV can be sufficient to support local demand (1,2). Higher  $^{99m}\text{Tc}$  yields can be obtained with medium-energy cyclotrons capable of accelerating protons up to 24 MeV. It was shown previously in theory (3) and empirically (4) that the yield doubles when incident energy increases from 16 to 24 MeV. To take advantage of higher production capacity of medium-energy cyclotrons, the quality of  $^{99m}\text{Tc}$  manufactured at higher energies and, in particular, its radioisotopic purity required detailed evaluation.

$^{99m}\text{Tc}$  is formed by irradiation of  $^{100}\text{Mo}$  targets via the  $^{100}\text{Mo}(p,2n)^{99m}\text{Tc}$  nuclear reaction. When thick targets are used, as in this work, the incident beam is significantly degraded in energy traversing the target material (5). Therefore, nuclear reactions occur over a range of energies starting with the incident energy ( $E_{\text{in}}$ ) of the proton and down to the outgoing energy ( $E_{\text{out}}$ ) when the particle exits the target. Other radionuclides are coproduced as a result of (p,pn), (p, $\alpha$ ), and (p, $\alpha$ n) reactions, namely molybdenum and niobium isotopes, and are easily separated from  $^{99m}\text{Tc}$  during target processing. Inherent isotopic contaminants in the  $^{100}\text{Mo}$  starting material also undergo nuclear transformations via (p,n), (p,2n), and (p,3n) into corresponding radionuclides giving rise to  $^{93m+g}\text{Tc}$ ,  $^{94m+g}\text{Tc}$ ,  $^{95m+g}\text{Tc}$ ,  $^{96m+g}\text{Tc}$ ,  $^{97m+g}\text{Tc}$ ,  $^{98}\text{Tc}$ , and  $^{99g}\text{Tc}$  isotopes. All technetium isotopes are chemically identical and cannot be separated during target chemical processing. As a result, the final formulation of the cyclotron-produced sodium pertechnetate  $^{99m}\text{Tc}$  will contain traces of other technetium

Received Mar. 4, 2015; revision accepted Jul. 15, 2015.

For correspondence or reprints contact: Svetlana V. Selivanova, 3001, 12th Ave. Nord, Sherbrooke, QC, J1H 5N4, Canada.

E-mail: [svetlana.v.selivanova@usherbrooke.ca](mailto:svetlana.v.selivanova@usherbrooke.ca)

Published online Jul. 23, 2015.

COPYRIGHT © 2015 by the Society of Nuclear Medicine and Molecular Imaging, Inc.

isotopes, which may contribute to an increase in patient dose and potentially affect image quality. Theoretic calculations on the extent of  $^{99m}\text{Tc}$  radioisotopic purity and experimental evaluation of cross sections on thin foils made of enriched molybdenum were conducted previously by others (3,4). This work evaluated the quality of sodium pertechnetate  $^{99m}\text{Tc}$  produced with a cyclotron starting from thick (0.58, 0.72, and 0.88 g/cm<sup>2</sup>)  $^{100}\text{Mo}$  targets. We present here experimental results of the irradiations at 20–24 MeV, including chemical, radiochemical, and radionuclidic purity of produced sodium pertechnetate  $^{99m}\text{Tc}$  and its imaging efficacy and explain initial grounds for proposed release specifications.

## MATERIALS AND METHODS

All commercially available reagents and solvents were used as received. High-purity water (Optima LC/MS, ultra-high performance liquid chromatography ultraviolet grade, 0.03  $\mu\text{m}$  filtered; Fisher Scientific) was used to prepare all buffer solutions. Generator-eluted  $^{99m}\text{Tc}$  was supplied in bulk vials by Lantheus Medical Imaging. Radioactivity measurements were performed in an ionization chamber (CRC-25PET; Capintec) on the  $^{99m}\text{Tc}$  setting to control process efficiency and by  $\gamma$ -ray spectrometry with a calibrated high-purity germanium detector (GMX HPGe; ORTEC) for analytic quantitation. Electron microscopy was performed at the Materials Characterization Centre of the Université de Sherbrooke.

### Target Fabrication

Coin-shaped targets were prepared using 2 batches (batch A and batch B) of  $^{100}\text{Mo}$  (ISOFLEX USA) with different enrichment and isotopic composition (Table 1). Interaction depth (target thickness in g/cm<sup>2</sup>) providing required proton-beam attenuation was calculated using SRIM software (6). The mass of  $^{100}\text{Mo}$  powder for each target was determined from the calculated target thickness and pellet geometry. The  $^{100}\text{Mo}$  metal powder was pressed into a groove of  $\phi$  6.35 mm in the middle of a coin-shaped aluminum backing measuring 24 mm in diameter and 2 mm thick. Pressing protocol was standardized as much as possible to produce a consistent-density pellet. The  $^{100}\text{Mo}$  packing density in pressed targets is different from crystal density for molybdenum (used in SRIM), but as long as target thickness in units of g/cm<sup>2</sup> remains unchanged, energy attenuation will be the same. Targets were prepared at the Laboratory of Materials Preparation and Characterization of the Brockhouse Institute for Materials Research, McMaster University, Ontario, Canada, according to the specifications provided above.

### Irradiation Conditions

Targets ( $n \geq 3$  per condition) were irradiated facing a perpendicular proton beam in a solid target holder mounted to a target selector installed directly on a TR-24 cyclotron (Advanced Cyclotron Systems Inc.). Irradiations were performed at an  $E_{\text{in}}$  of 20, 22, and 24 MeV. The collimated proton beam was 10 mm in diameter. A target current of 15  $\mu\text{A}$  was applied during 2-h irradiations, whereas 6-h runs were performed with 5  $\mu\text{A}$  to achieve comparable integrated current. Batch A targets reached the integrated current of  $1,882 \pm 28$ ,  $1,811 \pm 10$ , and  $1,727 \pm 29$   $\mu\text{A}\cdot\text{min}$  at an  $E_{\text{in}}$  of 20, 22, and 24 MeV, respectively. Batch B targets reached  $1,898 \pm 70$   $\mu\text{A}\cdot\text{min}$  at an  $E_{\text{in}}$  of 24 MeV.

### Target Processing and $^{99m}\text{Tc}$ -Pertechnetate Purification

Processing of the target solute was performed following a published procedure (7) with some modifications. Instead of sodium hydroxide, ammonia carbonate solution (2.5 M) was used to load the separation column and sodium carbonate (1 M) to rinse it. In addition, load/elution flow direction was not reversed. The detailed description can be found in the supplemental data (supplemental materials are available at <http://jnm.snmjournals.org>).

Relative isolated radiochemical yield ( $^{99m}\text{Tc}$  radioactivity as a fraction of all radioactivity originally present) was calculated on the basis of the total radioactivity recovered after processing. Recovered radioactivity in this case is the sum of the measurements of all postprocessing radioactive materials, for example, the product vial with sodium pertechnetate  $^{99m}\text{Tc}$ ; target solute containing  $^{99}\text{Mo}$ ,  $^{96}\text{Nb}$ ,  $^{97}\text{Nb}$ , and potentially nontrapped technetium isotopes; and cartridges with resins as measured in an ionization chamber on the  $^{99m}\text{Tc}$  setting.

The process efficiency was calculated as a fraction of  $^{99m}\text{Tc}$  radioactivity in the product vial to total recovered  $^{99m}\text{Tc}$  radioactivity after processing, namely, the product vial with sodium pertechnetate  $^{99m}\text{Tc}$ , cartridges with resins, and waste vial.

### Analytic Procedures

Chemical purity in the final formulation was evaluated semi-quantitatively using commercially available indicator strips to measure trace amounts of aluminum (Tec-Control [Biodex]; detection limit, 10  $\mu\text{g/mL}$ ), molybdenum (EM Quant Molybdenum Test [EMD]; detection limit, 5  $\mu\text{g/mL}$ ), ammonia (Quantofix Ammonium [Macherey-Nagel]; detection limit, 10  $\mu\text{g/mL}$ ), and hydrogen peroxide (Quantofix Peroxide [Macherey-Nagel]; detection limit, 0.5  $\mu\text{g/mL}$ ).

Radiochemical identity and purity of the final product were determined by thin-layer chromatography. Thin-layer chromatography plates with a silica gel matrix (4  $\times$  8 cm, polyethylene terephthalate support; Fluka) were developed in acetone (Sigma-Aldrich). Radioactivity was quantified using an InstantImager A2024 digital autoradiograph (Canberra Packard) or AR-2000 scanner (Bioscan).

Radiochemical stability was evaluated in sterile pyrogen-free vials in upright and inverted position up to 24 h after the formulation. For this, the determination of radiochemical identity and purity was performed according to the thin-layer chromatography procedure described above.

Radionuclidic identity was confirmed by  $\gamma$ -ray spectrometry (the most prominent  $\gamma$  ray of  $^{99m}\text{Tc}$  has an energy of 140.5 keV) and by measuring the product's radioactivity half-life in an ionization chamber. For the half-life, the radioactivity of the sample was measured after completion of the formulation (arbitrary time  $t_0$ , 3–4 h after the end of bombardment [EOB]) and remeasured again at another time point  $t$  (at least 36 min, which is 10% of the  $^{99m}\text{Tc}$  half-life and up to 30 h).

### Quantitative Determination of Radionuclidic/Radioisotopic Impurities

Radionuclidic or radioisotopic purity was determined using  $\gamma$ -ray spectrometry and decay corrected to the EOB. The procedure is described in detail in the supplemental data. Test samples originated

**TABLE 1**  
Isotopic Composition of  $^{100}\text{Mo}$  Targets

Batch	$^{100}\text{Mo}$	$^{98}\text{Mo}$	$^{97}\text{Mo}$	$^{96}\text{Mo}$	$^{95}\text{Mo}$	$^{94}\text{Mo}$	$^{92}\text{Mo}$
A	99.03	0.54	0.08	0.11	0.09	0.07	0.08
B	99.815	0.17	0.003	0.003	0.003	0.003	0.003

from formulated sodium pertechnetate as well as from target solute before and after pertechnetate extraction. A test sample of formulated sodium pertechnetate was assayed at 3, 6, 9, 12, and 24 h after the EOB, and decay-corrected measured values were averaged. The samples were also assayed at approximately 1, 2, and 4 wk after production to quantify long-lived isotopes (e.g.,  $^{95m}\text{Tc}$  and  $^{97m}\text{Tc}$ ). For target solute, additional corrections were applied to the counts registered at 140.5 keV as described elsewhere (8,9).

### Assessment of Internal Radiation Dose

The estimation of internal dose was based on the experimentally measured radioisotopic composition of each technetium isotope at a certain time (EOB and potential injection time of 3, 4, 5, 6, 9, 12, 15, 18, and 24 h after the EOB). The biokinetic model for  $^{99m}\text{Tc-NaTcO}_4$  in humans (intravenous administration, no blocking agent) described in International Commission on Radiological Protection publication 53 (10) was used to calculate the effective dose for  $^{99m}\text{Tc}$ . Published time-integrated activity coefficients ( $\tilde{a}$ ) for other technetium isotopes in the form of pertechnetate (11) were applied to calculate the internal dose that would result from each technetium isotope if injected individually. The dose for each isotope was multiplied by its fraction in the solution of sodium pertechnetate at a tentative time of injection, and partial doses due to each isotope were added together. The calculations were performed using OLINDA/EXM software (12).

### Phantom Imaging

Phantom imaging of sodium pertechnetate  $^{99m}\text{Tc}$  was performed using cyclotron-produced  $^{99m}\text{Tc}$  ( $E_{\text{in}} = 24$  MeV, 2-h irradiation, 99.815%  $^{100}\text{Mo}$ ) and commercially available  $^{99m}\text{Tc}$  from a generator up to 18 h after the end of production/elution. Planar and SPECT images were acquired on a Discovery NM/CT 670 SPECT/CT camera (GE Healthcare) equipped with low-energy high-resolution collimators. The energy window was  $140.5 \text{ keV} \pm 7.5\%$ . SPECT acquisition with a capillary phantom was performed with a constant rotation radius of 23 cm, 120 projections, 18 s/projection, and  $3^\circ$  angular step and reconstructed using a filtered backprojection algorithm ( $128 \times 128$  matrix, ramp filter). A capillary phantom (Capilets glass capillary microhematocrit tube; Dade Division, American Hospital Supply Corporation) was used for planar and SPECT imaging. The Jaszczak phantom filled with water (Jaszczak Flangeless Deluxe SPECT Phantom [Biodex]; cold rod diameters, 4.8, 6.4, 7.9, 9.5, 11.1, and 12.7 mm; cylinder interior dimensions,  $\phi 20.4 \times 18.6$  cm) was used for planar imaging only. The phantom was positioned vertically on top of the camera collimator. The images with  $^{99m}\text{Tc}$  eluted from a generator (730 MBq,  $n = 2$ ) or  $^{99m}\text{Tc}$  produced using a cyclotron (620–746 MBq, at 5, 7.5, 9, 11, 13, 15, and 17 h after the EOB,  $n = 1$  at each time point) were acquired for 4–5 min to reach comparable total number of counts. Image contrast and contrast-to-noise ratio (CNR) were calculated using the following equations:

$$\text{Contrast} = \frac{R_{\text{hot}} - R_{\text{cold}}}{R_{\text{cold}}};$$

$$\text{CNR} = \frac{\frac{R_{\text{hot}} - R_{\text{cold}}}{R_{\text{cold}}}}{\sqrt{\left(\frac{\sigma_{\text{hot}}}{R_{\text{hot}}}\right)^2 + \left(\frac{\sigma_{\text{cold}}}{R_{\text{cold}}}\right)^2}},$$

where  $R_i$  is expressed in counts per second per pixel and  $\sigma_i$  is SD. The  $R_{\text{cold}}$  values were determined by averaging the background counting rates in the largest (12.7 mm) cold spots, whereas the  $R_{\text{hot}}$  values were estimated in a large region of interest surrounding the cold spots.

## RESULTS

### Target Fabrication

Calculated and actual  $^{100}\text{Mo}$  targets parameters are shown in Table 2. Because of a slightly higher molybdenum mass than required for targets prepared for an energy drop of  $22 \rightarrow 10$  MeV, actual attenuation was to  $9.1 \pm 0.2$  MeV.

### Target Dissolution and $^{99m}\text{Tc}$ -Pertechnetate Purification

Irradiation conditions and target radioactivity measured at retrieval ( $\sim 1$  h after the EOB) are described in Table 3. The radioactivity measurement of the target before and after processing (80- to 90-min time difference, not decay corrected) showed that 50%–65% of the radioactivity did not dissolve and remained on the target, which was also confirmed by measuring nondissolved target mass after decay (Table 3). The measured values are arbitrary, because a range of other radionuclides (technetium, niobium, and molybdenum isotopes) are present in an irradiated target and produce a different response of the ionization chamber detector. The relative isolated radiochemical yield (the efficiency of separation from other radionuclides) of sodium pertechnetate was in a range of 66%–86% and depended on proton incident energy (Table 3). Four to seven percent of the radioactivity was distributed between cartridges and washing effluent. The remaining radioactivity (10%–30%, overestimated because radionuclides with higher  $\gamma$ -ray energies than  $^{99m}\text{Tc}$  produce a higher reading in an ionization chamber on the  $^{99m}\text{Tc}$  setting) was found in the vial with processed target solute, which contained a mixture of  $^{99}\text{Mo}$ ,  $^{96}\text{Nb}$ , and  $^{97}\text{Nb}$ . Although these values are arbitrary, they give the ability to follow the radioactivity flow during the separation process. Of the total  $^{99m}\text{Tc}$  radioactivity,  $93\% \pm 2\%$  was found in the product vial,  $3.1\% \pm 0.9\%$  remained trapped on the separation column,  $2.1\% \pm 0.8\%$  was lost to the purification resins, and less than 1% was found in the waste vial.

### Quality Control

Solutions of sodium pertechnetate  $^{99m}\text{Tc}$  formulated for injection had a pH of 5.0–5.5 and contained greater than 98% of

**TABLE 2**  
 $^{100}\text{Mo}$  Targets Characteristics

Energy drop (MeV)	Molybdenum crystal density (g/cm <sup>3</sup> )	Thickness of molybdenum layer at crystal density (mm)	Calculated thickness of molybdenum layer (g/cm <sup>2</sup> )	Calculated molybdenum mass (mg)	Actual molybdenum mass (mg)	Calculated $E_{\text{out}}$ (MeV)
20→10	10.206	0.564	0.58	182.2	$179.9 \pm 0.6$	$10.2 \pm 0.1$
22→10	10.206	0.709	0.72	229.0	$241.2 \pm 3.2$	$9.1 \pm 0.2$
24→10	10.206	0.865	0.88	279.4	$280.7 \pm 2.2$	$9.9 \pm 0.2$

**TABLE 3**  
Target Irradiation Conditions and Processing Results

$E_{in}$ (MeV)	Calculated $E_{out}$ (MeV)	Irradiation time (min)	Integrated current ( $\mu$ A·min)	Molybdenum enrichment (%)	Target activity at retrieval (~1 h after EOB) (GBq)	Dissolved fraction (by mass) (%)	$E_{out}$ based on dissolved fraction (MeV)	$^{99m}\text{Tc}$ relative isolated yield* (%)
20	10.2 $\pm$ 0.1	133 $\pm$ 13	1,882 $\pm$ 28	99.03	9.2 $\pm$ 0.2	51.9 $\pm$ 0.5	15.50 $\pm$ 0.04	84.5 $\pm$ 1.8
22	9.1 $\pm$ 0.2	123 $\pm$ 2	1,811 $\pm$ 10	99.03	10.2 $\pm$ 0.4	35 $\pm$ 6	18 $\pm$ 1	77.0 $\pm$ 4.7
24	9.7 $\pm$ 0.1	121 $\pm$ 1	1,709 $\pm$ 32	99.03	9.7 $\pm$ 1.1	42 $\pm$ 6	18 $\pm$ 2	71.9 $\pm$ 5.8
24	9.8 $\pm$ 0.1	361 $\pm$ 2	1,744 $\pm$ 13	99.03	7.85 $\pm$ 0.05	38 $\pm$ 11	20 $\pm$ 1	67.8 $\pm$ 1.7
24	10.04 $\pm$ 0.06	122 $\pm$ 5	1,946 $\pm$ 141	99.815	9.8 $\pm$ 0.8	43 $\pm$ 9	19 $\pm$ 1	70.2 $\pm$ 3.7

\*Based on dissolved and recovered radioactivity at end of synthesis; not to be mistaken for absolute yield of nuclear reaction.

**TABLE 4**  
Radionuclidic Composition (%) of Target Solute as Function of Irradiation Energy\*

Nuclide	20 MeV	22 MeV	24 MeV
$^{99m}\text{Tc}$	90.2 $\pm$ 0.8	87.23 $\pm$ 0.02	86 $\pm$ 2
$^{97m}\text{Tc}$	0.0011 $\pm$ 0.0003	0.0010 $\pm$ 0.0002	0.0011 $\pm$ 0.0009
$^{96}\text{Tc}$	0.063 $\pm$ 0.001	0.13 $\pm$ 0.01	0.14 $\pm$ 0.05
$^{95}\text{Tc}$	0.087 $\pm$ 0.001	0.108 $\pm$ 0.006	0.2 $\pm$ 0.2
$^{95m}\text{Tc}$	0.00049 $\pm$ 0.00002	0.0005 $\pm$ 0.0001	0.0006 $\pm$ 0.0001
$^{94}\text{Tc}$	0.147 $\pm$ 0.001	0.201 $\pm$ 0.005	0.19 $\pm$ 0.02
$^{93}\text{Tc}$	0.18 $\pm$ 0.03	0.26 $\pm$ 0.02	0.2 $\pm$ 0.1
$^{99}\text{Mo}$	2.7 $\pm$ 0.2	4.7 $\pm$ 0.4	5 $\pm$ 1
$^{97}\text{Nb}$	6.3 $\pm$ 0.5	6.6 $\pm$ 0.2	6.6 $\pm$ 0.6
$^{96}\text{Nb}$	0.32 $\pm$ 0.05	0.78 $\pm$ 0.09	0.8 $\pm$ 0.3

\* $\gamma$ -spectrometry measurements (decay corrected to EOB) for batch A  $^{100}\text{Mo}$  targets irradiated for 2 h.

radioactivity in the form of pertechnetate ion. The product was stable for at least 24 h after its formulation. The half-life measured up to 24 h after the EOB was in a range of 5.87–6.09 h ( $^{99m}\text{Tc}$  half-life is 6.015 h (13)). Concentration of the aluminum, molybdenum, and ammonium were below the detection limit of the used commercial test kits, that is, less than 10  $\mu\text{g/mL}$  for aluminum, less than 5  $\mu\text{g/mL}$  for molybdenum, and less than 10  $\mu\text{g/mL}$  for ammonium. Hydrogen

peroxide was detected in some batches at a concentration between 0.5 and 2  $\mu\text{g/mL}$ , with a detection limit of 0.5  $\mu\text{g/mL}$ .

#### Determination of Radioisotopic and Radionuclidic Purity

The radionuclidic composition of the target solute for batch A of  $^{100}\text{Mo}$  at different irradiation conditions measured by  $\gamma$ -ray spectrometry is shown in Table 4. An increase in efficiency of the  $^{100}\text{Mo}(\text{p,pn})^{99}\text{Mo}$  reaction was notable when shifting to higher irradiation energy.

No breakthrough of coproduced  $^{99}\text{Mo}$ ,  $^{96}\text{Nb}$ , or  $^{97}\text{Nb}$  was detected in the purified sodium pertechnetate across all the experiments. We did not detect metastable  $^{93m}\text{Tc}$  and  $^{94m}\text{Tc}$  as predicted by theoretic calculations, probably because of their low content and short half-life (Supplemental Table 1). The quantification of  $^{96m}\text{Tc}$  was not possible because of its short half-life, low  $\gamma$ -ray intensity, and the overlapping  $\gamma$ -ray signature with its ground-state counterpart  $^{96}\text{Tc}$ . Therefore, all counts at 812.5 keV were assigned to  $^{96}\text{Tc}$ . Technetium isotopes, namely  $^{93}\text{Tc}$ ,  $^{94}\text{Tc}$ ,  $^{95}\text{Tc}$ ,  $^{95m}\text{Tc}$ ,

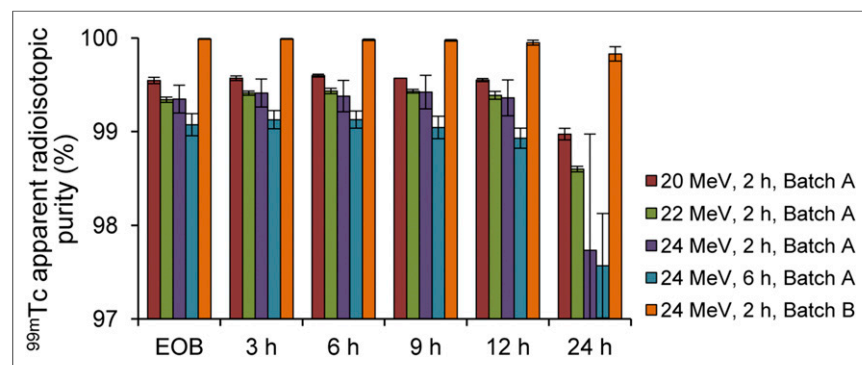


**FIGURE 1.** Apparent radioisotopic purity of sodium pertechnetate  $^{99m}\text{Tc}$  produced at different irradiation parameters as function of time after EOB.



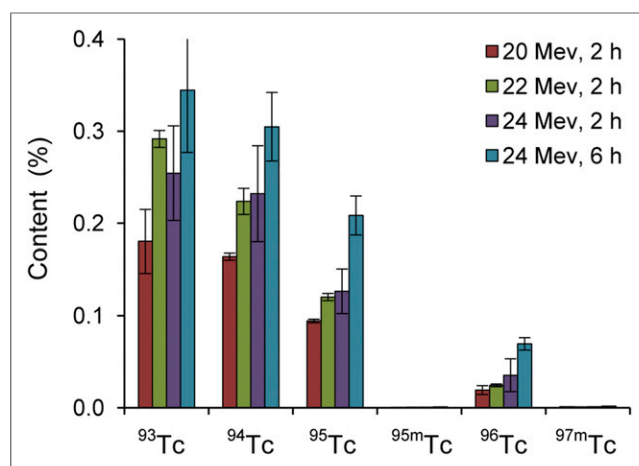


**FIGURE 2.** Profile of radioisotopic impurities in sodium pertechnetate  $^{99m}\text{Tc}$  from batch A  $^{100}\text{Mo}$  targets as function of irradiation energy and irradiation time. Content is expressed as percentage of radioactivity due to a given isotope to total radioactivity in sample.

$^{96}\text{Tc}$ , and  $^{97m}\text{Tc}$ , were detected along with  $^{99m}\text{Tc}$  when produced from batch A molybdenum targets. The radioisotopic purity of  $^{99m}\text{Tc}$  exceeded 99.0% (range, 99.1%–99.5%; decay-corrected EOB) (Fig. 1). The quantity of radioisotopic contaminants was dependent on irradiation energy and irradiation time (Fig. 2). For batch B  $^{100}\text{Mo}$  targets irradiated at an  $E_{\text{in}}$  of 24 MeV for 2 h, only trace amounts of  $^{95m}\text{Tc}$  ( $<0.00001\%$ ),  $^{96}\text{Tc}$  ( $\sim 0.01\%$ ), and  $^{97m}\text{Tc}$  ( $<0.001\%$ ) were detected, resulting in an apparent radioisotopic purity of  $^{99m}\text{Tc}$  of 99.98% or more (decay-corrected EOB) (Table 5). Because of low trace levels, detection of longer-lived  $^{95m}\text{Tc}$  and  $^{97m}\text{Tc}$  was possible only by measuring the full product vial after complete decay of  $^{99m}\text{Tc}$  and partial decay of  $^{96}\text{Tc}$  (at least 2 wk after EOB).

#### Assessment of Internal Radiation Dose

Figure 3 shows the estimated radiation dose increase for sodium pertechnetate  $^{99m}\text{Tc}$  produced from both batches of molybdenum under different irradiation conditions relative to pure  $^{99m}\text{Tc}$  (without any radionuclidic impurities) and how it changes depending on the time of injection after the EOB. The internal dose to target

organs is exemplified for a tentative injection time of 6 h after EOB (Table 6).

#### Phantom Imaging

For a capillary phantom filled with sodium pertechnetate  $^{99m}\text{Tc}$  eluted from a generator, planar image resolution in full width at half maximum was  $4.15 \pm 0.05$  mm at 0 cm and  $6.82 \pm 0.04$  mm at 10 cm from the  $\gamma$ -camera collimator. The resolution of images with cyclotron-produced  $^{99m}\text{Tc}$  ( $E_{\text{in}} = 24$  MeV, 2-h irradiation, 99.815%  $^{100}\text{Mo}$ ) was  $4.21 \pm 0.06$  mm when the capillary was positioned at 0 cm from the collimator and  $6.83 \pm 0.09$  mm at 10 cm. In both cases, the resolution remained stable in time, within measurement error (Fig. 4). In SPECT, full width at half maximum for the capillary filled with generator sodium pertechnetate  $^{99m}\text{Tc}$  was 14.47 mm at 0 cm and 14.39 mm at 9 cm from the center of rotation (single measurements). The resolution of images with cyclotron-produced  $^{99m}\text{Tc}$  was the same ( $14.45 \pm 0.12$  mm) when the capillary was positioned at 0 cm from the center of rotation and insignificantly degraded to  $14.55 \pm 0.12$  mm at 9 cm.

Planar images acquired using the Jaszczak phantom were of comparable quality without significant loss in spatial resolution (Fig. 5). On average, the contrast of images acquired using cyclotron-produced  $^{99m}\text{Tc}$  ( $E_{\text{in}} = 24$  MeV, 2-h irradiation, 99.815%  $^{100}\text{Mo}$ ) up to 17 h after the EOB ( $n = 7$ ) was  $1.16 \pm 0.02$  with a CNR of  $10.47 \pm 0.26$ , which compares favorably to the best of 2 values obtained for generator-eluted  $^{99m}\text{Tc}$ : 1.14 (contrast) and 10.28 (CNR).

#### DISCUSSION

The main distinguishing difference between cyclotron-produced  $^{99m}\text{Tc}$  and generator-eluted  $^{99m}\text{Tc}$  is that cyclotron-produced  $^{99m}\text{Tc}$  is contaminated with other technetium isotopes (Table 4). This may contribute to additional radiation dose to patients and affect image resolution and contrast. Before direct manufacturing of  $^{99m}\text{Tc}$  using cyclotrons becomes routine, there is a necessity to acquire sufficient supporting data about the quality of the cyclotron-produced sodium pertechnetate  $^{99m}\text{Tc}$  and establish

**TABLE 5**

Radioisotopic Composition (%) of Cyclotron-Produced\* Sodium Pertechnetate

Nuclide	$^{100}\text{Mo}$ batch A ( $n = 4$ )	$^{100}\text{Mo}$ batch B ( $n = 7$ )
$^{99m}\text{Tc}$	$99.35 \pm 0.15$	$99.9896 \pm 0.0035$
$^{97m}\text{Tc}$	$0.0011 \pm 0.0009$	$0.00060 \pm 0.00008$
$^{96}\text{Tc}$	$0.035 \pm 0.017$	$0.0098 \pm 0.0035$
$^{95}\text{Tc}$	$0.127 \pm 0.024$	< detection limit
$^{95m}\text{Tc}$	$0.00059 \pm 0.00007$	$0.0000067 \pm 0.0000007$
$^{94}\text{Tc}$	$0.23 \pm 0.05$	< detection limit
$^{93}\text{Tc}$	$0.25 \pm 0.05$	< detection limit

\*Irradiation conditions: 24 MeV, 2 h; decay corrected to EOB.

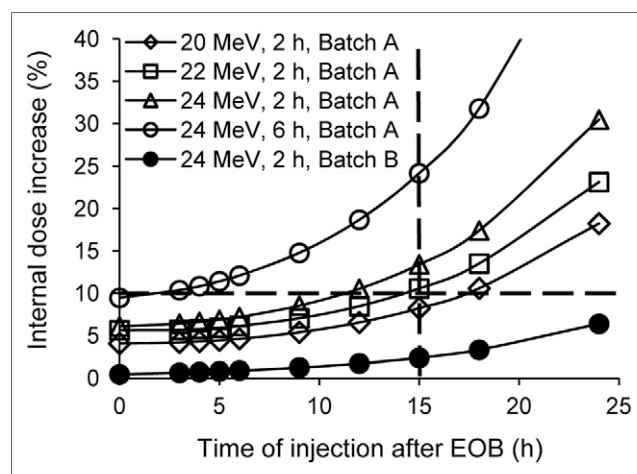


**FIGURE 3.** Estimated internal dose increase compared with pure  $^{99m}\text{Tc}$ . Horizontal dashed line is tentative 10% cutoff for potentially accepted dose increase. Vertical dashed line is a tentative shelf-life for sodium pertechnetate  $^{99m}\text{Tc}$  injection after end of synthesis (12-h end of synthesis = 15-h EOB).

**TABLE 6**  
Internal Dose (mSv/MBq) to Organs Assuming Injection Time of 6 Hours After EOB\*

Organ/tissue	$^{99m}\text{Tc-NaTcO}_4$ from $^{100}\text{Mo}^*$ batch A (99.03%)	$^{99m}\text{Tc-NaTcO}_4$ from $^{100}\text{Mo}^*$ batch B (99.815%)	$^{99m}\text{Tc-NaTcO}_4$ without any radionuclidic impurities
Adrenals	3.59E-03	3.32E-03	3.28E-03
Brain	2.10E-03	1.95E-03	1.93E-03
Breasts	1.83E-03	1.68E-03	1.66E-03
Gallbladder wall	6.38E-03	5.93E-03	5.87E-03
Lower large intestine wall	2.20E-02	2.06E-02	2.04E-02
Small intestine	1.64E-02	1.56E-02	1.55E-02
Stomach wall	1.18E-02	1.13E-02	1.12E-02
Upper large intestine wall	2.88E-02	2.75E-02	2.73E-02
Heart wall	3.12E-03	2.89E-03	2.85E-03
Kidneys	4.05E-03	3.74E-03	3.70E-03
Liver	3.61E-03	3.33E-03	3.29E-03
Lungs	2.62E-03	2.43E-03	2.40E-03
Muscle	3.22E-03	2.97E-03	2.93E-03
Ovaries	9.66E-03	8.84E-03	8.72E-03
Pancreas	5.01E-03	4.66E-03	4.61E-03
Red marrow	3.57E-03	3.26E-03	3.22E-03
Osteogenic cells	7.47E-03	7.20E-03	7.16E-03
Skin	1.86E-03	1.71E-03	1.69E-03
Spleen	3.96E-03	3.67E-03	3.63E-03
Testes	2.99E-03	2.74E-03	2.70E-03
Thymus	2.56E-03	2.36E-03	2.33E-03
Thyroid	2.23E-02	2.17E-02	2.16E-02
Urinary bladder wall	1.76E-02	1.66E-02	1.65E-02
Uterus	8.19E-03	7.58E-03	7.50E-03
Total body	3.57E-03	3.31E-03	3.27E-03
Effective dose equivalent	1.01E-02	9.51E-03	9.42E-03
Effective dose	9.93E-03	9.34E-03	9.26E-03

\*Irradiation conditions: 24 MeV, 2 h.

a regulatory framework for its use in clinical practice. Because absolute production yields increase with higher energies, it would be advantageous to use the highest practical energy (24 MeV with TR-24 cyclotron), making the manufacturing process shorter and more cost-effective per hour of manufacturing time. Therefore, we evaluated the quality of the sodium pertechnetate  $^{99m}\text{Tc}$  produced with a cyclotron at medium energies ( $E_{\text{in}} = 20\text{--}24$  MeV), including its radioisotopic purity, and assessed the results with respect to internal radiation dose and image quality.

A limitation of the current study is that the irradiated target material did not dissolve completely. Low surface area of the reaction and relatively high metrical thickness seem to be the main reasons. To investigate the extent of dissolution, after approximately 10 mo of decay, the targets were taken apart (Supplemental Fig. 2), and the remaining  $^{100}\text{Mo}$  pellets were weighed (Table 3) and inspected under an electron microscope. Because the erosion depth of the remaining target material is rather uniform (Supplemental Fig. 3), we assume that the dissolved target thickness is also uniform. Analyzing the cross sections for  $^{99m}\text{Tc}$  and coproduced radionuclides (3) together with potential dose from each

technetium isotope if injected individually (Supplemental Table 2), we demonstrated that the results presented in this work are a conservative estimation of the radioisotopic purity. One could

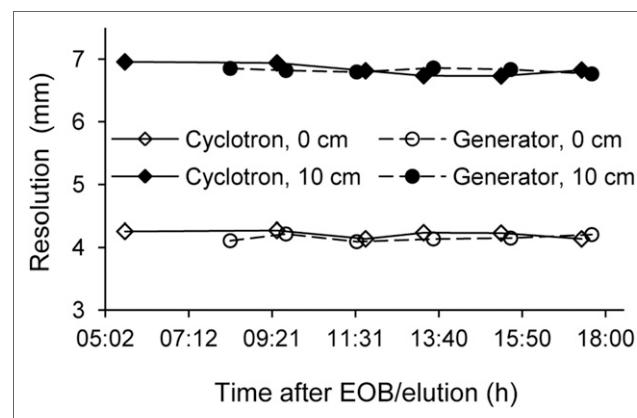


**FIGURE 4.** Full width at half maximum resolution of planar capillary images with cyclotron- and generator-produced sodium pertechnetate  $^{99m}\text{Tc}$ .

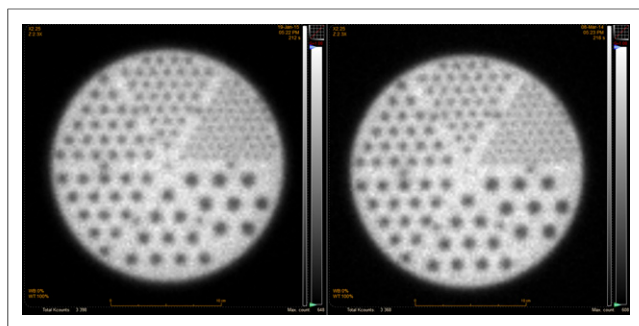


**FIGURE 5.** Images of Jaszczak phantom filled with solution of sodium pertechnetate  $^{99m}\text{Tc}$ . (Left) Eluted from generator. (Right) Cyclotron-produced. Images are on linear gray scale with white being equal to maximum intensity. Cold rods are 4.8, 6.4, 7.9, 9.5, 11.1, and 12.7 mm in diameter.

observe that  $^{94}\text{Tc}$ ,  $^{95m}\text{Tc}$ ,  $^{95}\text{Tc}$ ,  $^{96}\text{Tc}$ , and  $^{97m}\text{Tc}$  contribute the most to the effective dose.  $^{94}\text{Tc}$ ,  $^{95m}\text{Tc}$ , and  $^{95}\text{Tc}$  are produced from  $^{94-97}\text{Mo}$ , each of which represents less than 0.003% of the initial target composition of high-purity  $^{100}\text{Mo}$  (batch B) material, resulting in a low amount of  $^{94}\text{Tc}$ ,  $^{95m}\text{Tc}$ , and  $^{95}\text{Tc}$  in the final product that can be considered negligible (Table 5).  $^{97m}\text{Tc}$  content is also rather low because reaction channels leading to this isotope have limited physical thick target yields (4). Therefore,  $^{96}\text{Tc}$  is the primary isotope responsible for the dose increase and potentially harmful to image quality because of its energetic  $\gamma$  rays. The main production route for  $^{96}\text{Tc}$  in batch B targets is  $^{98}\text{Mo}(p,3n)^{96}\text{Tc}$  nuclear reaction, which starts to occur at a proton beam above 20 MeV. The dissolved top layer of the target surface will contain the higher proportion of  $^{96}\text{Tc}$  relative to  $^{99m}\text{Tc}$  than the rest of the target, where proton energy degraded to less than 20 MeV, and this reaction does not happen anymore, which is exemplified by Figure 6. For batch B targets irradiated at an  $E_{\text{in}}$  of 24 MeV, actual  $E_{\text{out}}$  for the dissolved fraction was  $19 \pm 1$  MeV as estimated from the dissolved target mass. It means that our current data overestimate relative  $^{96}\text{Tc}$  content compared with fully dissolved target (Fig. 6). In addition, according to previously published calculations (3), the

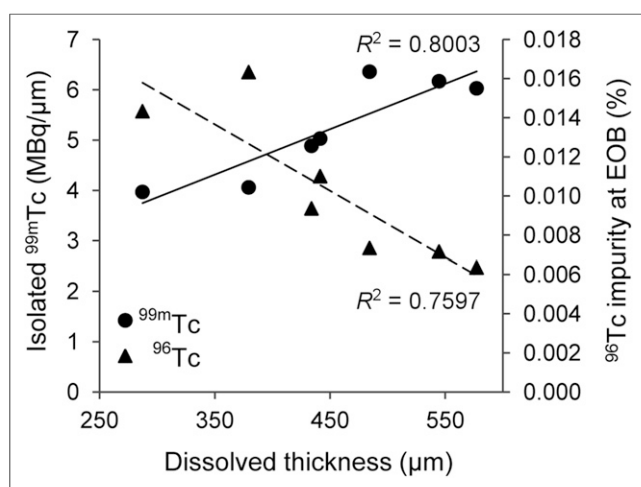


**FIGURE 6.** For energy attenuation of  $24 \rightarrow 19 \pm 1$  MeV, relative isolated yield of  $^{99m}\text{Tc}$  increases with dissolved target depth. Content of  $^{96}\text{Tc}$ , on contrary, is decreasing.

individual ratios of contaminants to  $^{99m}\text{Tc}$  are the most advantageous below the threshold of 19 MeV. Therefore, the results reported here exemplify the less favorable energy region for  $^{99m}\text{Tc}$  production ( $24 \rightarrow 19$  MeV) and can serve as a reasonable worst-case approximation.

Polyethylene glycol-based aqueous biphasic extraction chromatography resin was selected for separation because it is known to retain pertechnetate from industrial alkaline waste (14) and was reported for separation of medical  $^{99m}\text{Tc}$  (15). A range of other resins of the same nature, namely the Tentagel (Rapp Polymere) and ChemMatrix (PCAS BioMatrix) product lines, were tested recently by others and showed similar results (16,17). We speculated that any resin with high enough polyethylene glycol load ( $\geq 2,000$ ) would perform sufficiently well.

Quality control of the formulated sodium pertechnetate  $^{99m}\text{Tc}$  confirmed that the compound's chemical and radiochemical purity conformed to the limits set by European and U.S. Pharmacopeias for the generator-eluted pertechnetate (Table 7). Among raw materials (aluminum, molybdenum, ammonium, and hydrogen peroxide), only hydrogen peroxide was above the detection limit in some batches ( $\leq 2 \mu\text{g/mL}$ ) if tested at the end of synthesis. Tests were negative when repeated after a few hours. All above-mentioned chemicals are biogenic and do not pose a toxic or pharmacologic hazard at low trace levels. Therefore, these tests, although performed as part of the process validation, may not be needed for daily quality control procedure.

The isotopic content of starting  $^{100}\text{Mo}$  is crucial for obtaining high-isotopic-purity  $^{99m}\text{Tc}$ . It was shown previously that irradiation of  $^{100}\text{Mo}$  with higher enrichment resulted in a product with lower radioisotopic purity than irradiation of lower enriched  $^{100}\text{Mo}$  with less  $^{92-97}\text{Mo}$  (11). Another factor responsible for the radionuclidic purity of cyclotron-produced  $^{99m}\text{Tc}$  is irradiation energy and time. The amount of produced isotopes depends on each radioisotope cross section and can be controlled by irradiation parameters as evidenced by Figure 2. Therefore, specifications for the target material based solely on  $^{100}\text{Mo}$  enrichment are not sufficient. Control of the isotopic composition of the starting material together with irradiation parameters is mandatory to guarantee radioisotopic purity of the final product.

For high-purity  $^{100}\text{Mo}$  (batch B) irradiated at 24 MeV for 2 h, virtually no radioisotopic impurities were found, with  $^{99m}\text{Tc}$  being 99.98% or more pure at the EOB and 99.95% or more during a tentative product shelf-life of 12 h after formulation. Current U.S. Pharmacopeia requires  $^{99m}\text{Tc}$  from a generator (fission) to be at least 99.96% pure as a radionuclide, whereas European Pharmacopeia expects 99.88% radioactivity due to  $^{99m}\text{Tc}$ . Depending on the  $^{99}\text{Mo}$  production method, both Pharmacopeias allow trace amounts of  $^{131}\text{I}$ ,  $^{103}\text{Ru}$ ,  $^{89}\text{Sr}$ ,  $^{90}\text{Sr}$ , and  $^{99}\text{Mo}$  to be present in sodium pertechnetate  $^{99m}\text{Tc}$ , in addition to some other  $\alpha$ - and  $\gamma$ -emitting radionuclidic impurities.

Because each isotope delivers a different radiation dose and its relative content in final formulation changes with time, we decided to devise specifications for radioisotopic purity based on a potential radiation dose increase compared with pure  $^{99m}\text{Tc}$ . The calculations were performed for several time points after EOB to reflect various injection times. It is postulated, conservatively, that a maximum 10% dose increase would be acceptable to nuclear medicine practitioners. On the basis of this assumption, one could select appropriate irradiation conditions for a given batch of enriched  $^{100}\text{Mo}$  target material to

**TABLE 7**  
Provisional Release Specifications for Sodium Pertechnetate  $^{99m}\text{Tc}$  Injection Manufactured with Cyclotron

Parameter/trace	Test method	Provisional specifications	Validation batches ( $n = 5$ )	European Pharmacopeia	U.S. Pharmacopeia
Appearance	Visual	Clear, colorless	Conform	Clear, colorless	—
pH	pH test strip	4.0–8.0	5.0–5.5	4.0–8.0	4.5–7.5
Radiochemical identity	Thin-layer chromatography	$R_f > 0.7^*$	0.8–0.9	$R_f \sim 0.6$	$R_f \sim 0.9\% \pm 10\%$
Radiochemical purity	Thin-layer chromatography	$\geq 95\%$	$> 98\%$	$\geq 95\%$	$\geq 95\%$
Radionuclidic identity	$\gamma$ -ray spectrometry	$\gamma$ ray at 141 keV	141 keV	140 keV	140 keV
Radioisotopic purity	$\gamma$ -ray spectrometry	$> 99.4\%$	$> 99.98\%$	$> 99.88\%$	$> 99.935\%$
Other nuclides (not technetium)	$\gamma$ -ray spectrometry	Undetectable $\gamma$ ray at 569, 658, 740 keV <sup>†</sup>	Conform	$\leq 0.12\%^{\ddagger}$	$\leq 0.065\%^{\ddagger}$

\*Validated for silica-gel/acetone system;  $R_f$  for sodium pertechnetate in other systems may be different.

<sup>†</sup> $\gamma$ -ray peaks correspond to  $^{96}\text{Nb}$  (569 keV),  $^{97}\text{Nb}$  (658 keV), and  $^{99}\text{Mo}$  (740 keV).

<sup>‡</sup>Trace amounts of  $^{99}\text{Mo}$ , as well as other nontechnetium radionuclides, are permitted in  $^{99m}\text{Tc}$  eluate.

fulfill this requirement. The shelf-life of the final product can also be adjusted on the basis of the radioisotopic purity of the final formulation. For example, according to our dosimetry assessment (Fig. 3), batch A of  $^{100}\text{Mo}$  must be irradiated at 20 MeV or less to produce an acceptable quality product with a shelf-life of 12 h after synthesis, whereas batch B can be used at any irradiation energy up to 24 MeV (inclusive), with a shelf-life potentially exceeding 24 h. Alternatively, batch A can be irradiated at higher energy, including 24 MeV, but the shelf-life of the product must be reduced accordingly, so that the radiation dose will not increase by more than 10%. As can be seen from Figure 3, sodium pertechnetate  $^{99m}\text{Tc}$  produced from batch A at 24 MeV, 2-h irradiation, could be used up to 12 h after irradiation (which is  $\sim 9$  h after formulation). The correlation of the variation of radioisotopic impurities in time with corresponding increase in effective dose for sodium pertechnetate (Fig. 3) allowed us to suggest that at least 99.4% of total radioactivity of the radiopharmaceutical drug product must be due to  $^{99m}\text{Tc}$  to remain inside the 10% limit for dose increase. However, this value will be different for other  $^{99m}\text{Tc}$  radiopharmaceuticals because biologic half-life and residence time in various organs differ among compounds, thus influencing absorbed dose.

The results of capillary phantom imaging with sodium pertechnetate  $^{99m}\text{Tc}$  produced from high-purity  $^{100}\text{Mo}$  (batch B) at 24 MeV for 2 h showed that the degradation of spatial resolution that may be due to the scattering of high-energy  $\gamma$  rays originating from isotopic impurities in cyclotron-produced  $^{99m}\text{Tc}$  is insignificant (Fig. 4) and is not expected to affect image definition and contrast. This was confirmed by the Jaszczak phantom studies, when the contrast and CNR of images acquired using cyclotron-produced  $^{99m}\text{Tc}$  compared favorably to the best of 2 values obtained for generator-eluted  $^{99m}\text{Tc}$ . Visually, 2 side-by-side images produced with  $^{99m}\text{Tc}$  from the generator and cyclotron were found to be equivalent by several experienced interpreters (Fig. 5).

Taking results together, we found the quality of sodium pertechnetate  $^{99m}\text{Tc}$  produced with a cyclotron at medium energies satisfactory and suitable for use in humans. All prepared batches were

tested, met provisional release specifications (Table 7), and complied with standard requirements for parenteral injections.

## CONCLUSION

We showed that the quality of  $^{99m}\text{Tc}$  produced with a cyclotron at medium energy can be fully adequate for clinical use provided that the isotopic composition of the starting molybdenum together with its irradiation parameters (energy, time) were selected appropriately. Analysis of the collected data allowed for drafting quality control protocols and release specifications as part of a clinical trial application. The clinical trial (ClinicalTrials.gov identifier NCT02307175; health authority, Health Canada) is ongoing; the outcome will be reported in due course. The results of this work are intended to contribute to establishing a regulatory framework for using cyclotron-produced  $^{99m}\text{Tc}$  in routine clinical practice.

## DISCLOSURE

The costs of publication of this article were defrayed in part by the payment of page charges. Therefore, and solely to indicate this fact, this article is hereby marked “advertisement” in accordance with 18 USC section 1734. This work was supported by Natural Resources Canada through the Isotope Technology Acceleration Program (ITAP). The Research Center of the Centre Hospitalier Universitaire de Sherbrooke (CRCHUS) is supported by the Fonds de recherche du Québec-Santé (FRQS). No other potential conflict of interest relevant to this article was reported.

## ACKNOWLEDGMENTS

We acknowledge our ITAP partners, University of Alberta and Advanced Cyclotron Systems Inc. We gratefully acknowledge Jim Garrett from the Laboratory of Materials Preparation and Characterization of the Brockhouse Institute for Materials Research, McMaster University, for preparing  $^{100}\text{Mo}$  targets and Charles Bertrand from the Materials Characterization Centre of the Université de Sherbrooke for producing images with the scanning electron microscope. We thank cyclotron operators Eric Berthelette and



Paul Thibault for providing excellent help with irradiations, René Ouellet for building automated dissolution/purification module, and Lidia Matei and Sébastien Tremblay for providing early experimentation with target processing. We are very grateful to Dr. Ondrej Lebeda for many helpful discussions.

## REFERENCES

- Guérin B, Tremblay S, Rodrigue S, et al. Cyclotron production of  $^{99m}\text{Tc}$ : an approach to the medical isotope crisis. *J Nucl Med*. 2010;51:13N–16N.
- Bénard F, Buckley KR, Ruth TJ, et al. Implementation of multi-Curie production of  $^{99m}\text{Tc}$  by conventional medical cyclotrons. *J Nucl Med*. 2014;55:1017–1022.
- Celler A, Hou X, Bénard F, Ruth T. Theoretical modeling of yields for proton induced reactions on natural and enriched molybdenum targets. *Phys Med Biol*. 2011;56:5469–5484.
- Lebeda O, van Lier EJ, Štursa J, Ráliš J, Zyuzin A. Assessment of radionuclidic impurities in cyclotron produced  $^{99m}\text{Tc}$ . *Nucl Med Biol*. 2012;39:1286–1291.
- Otuka N, Takacs S. Definitions of radioisotope thick target yields. *Radiochim Acta*. 2015;103:1–6.
- Ziegler JF, Ziegler MD, Biersack JP. The stopping and range of ions in matter. Version SRIM-2008.04. SRIM website. <http://www.srim.org/>. Accessed August 16, 2015.
- McAlister DR, Horwitz EP. Automated two column generator systems for medical radionuclides. *Appl Radiat Isot*. 2009;67:1985–1991.
- Gagnon KM. *Cyclotron Production of Technetium-99m* [PhD thesis]. Edmonton, Canada: University of Alberta; 2012.
- Gagnon K, Bénard F, Kovacs M, et al. Cyclotron production of  $^{99m}\text{Tc}$ : experimental measurement of the  $^{100}\text{Mo}(p,x)^{99}\text{Mo}$ ,  $^{99m}\text{Tc}$  and  $^{99g}\text{Tc}$  excitation functions from 8 to 18 MeV. *Nucl Med Biol*. 2011;38:907–916.
- International Commission on Radiological Protection. Radiation dose to patients from radiopharmaceuticals. ICRP publication 53. *Ann ICRP*. 1988; 18:197–200.
- Hou X, Celler A, Grimes J, Bénard F, Ruth T. Theoretical dosimetry estimations for radioisotopes produced by proton-induced reactions on natural and enriched molybdenum targets. *Phys Med Biol*. 2012;57:1499–1515.
- Stabin MG, Sparks RB, Crowe E. OLINDA/EXM: the second-generation personal computer software for internal dose assessment in nuclear medicine. *J Nucl Med*. 2005;46:1023–1027.
- Nuclear structure and decay data NuDat 2.5. Interactive Chart of Nuclides. 2011. Brookhaven National Laboratory National Nuclear Data Center website. <http://www.nndc.bnl.gov/nudat2/>. Accessed August 16, 2015.
- Rogers RD, Griffin ST, Horwitz EP, Diamond H. Aqueous biphasic extraction chromatography (ABEC): uptake of pertechnetate from simulated Hanford tank wastes. *Solvent Extr Ion Exch*. 1997;15:547–562.
- Rogers RD, Bond AH, Zhang J, Horwitz P. New technetium-99m generator technologies utilizing polyethylene glycol-based aqueous biphasic systems. *Sep Sci Technol*. 1997;32:867–882.
- Andersson J, Wilson J, Thomas B, et al. Tentagel® as chromatography media for processing cyclotron produced  $^{99m}\text{Tc}$  [abstract]. *J Nucl Med*. 2014;55(suppl 1):1248.
- Bénard F, Zeisler SK, Vuckovic M, et al. Cross-linked polyethylene glycol beads to separate  $^{99m}\text{Tc}$ -pertechnetate from low-specific-activity molybdenum. *J Nucl Med*. 2014;55:1910–1914.



The Journal of  
NUCLEAR MEDICINE

## Radioisotopic Purity of Sodium Pertechnetate $^{99m}\text{Tc}$ Produced with a Medium-Energy Cyclotron: Implications for Internal Radiation Dose, Image Quality, and Release Specifications

Svetlana V. Selivanova, Éric Lavallée, Helena Senta, Lyne Caouette, Jayden A. Sader, Erik J. van Lier, Alexander Zyuzin, Johan E. van Lier, Brigitte Guérin, Éric Turcotte and Roger Lecomte

*J Nucl Med.* 2015;56:1600-1608.

Published online: July 23, 2015.

Doi: 10.2967/jnumed.115.156398

---

This article and updated information are available at:

<http://jnm.snmjournals.org/content/56/10/1600>

---

Information about reproducing figures, tables, or other portions of this article can be found online at:

<http://jnm.snmjournals.org/site/misc/permission.xhtml>

Information about subscriptions to JNM can be found at:

<http://jnm.snmjournals.org/site/subscriptions/online.xhtml>

*The Journal of Nuclear Medicine* is published monthly.  
SNMMI | Society of Nuclear Medicine and Molecular Imaging  
1850 Samuel Morse Drive, Reston, VA 20190.  
(Print ISSN: 0161-5505, Online ISSN: 2159-662X)

© Copyright 2015 SNMMI; all rights reserved.